PERGAMON

International Journal of Solids and Structures 37 (2000) 4763–4781

INTERNATIONAL JOURNAL OF SOLIDS and STRUCTURES

www.elsevier.com/locate/ijsolstr

A statistical model for predicting effective electroelastic properties of polycrystalline ferroelectric ceramics with aligned defects

Jinquan Cheng*, Biao Wang, Shanyi Du

Research Center for Composite Materials, Harbin Institute of Technology, Harbin, 150001, People's Republic of China

Received 1 July 1998; in revised form 30 March 1999

Abstract

This work is focused on the analysis of the effects of domain switching and defects on the effective electroelastic properties of polycrystalline ferroelectric ceramics. On the basis of experimental results and the classical nucleation theory, a statistical micromechanics model is developed in order to describe the microstructural evolution of polycrystalline ferroelectric ceramics. Further, the methods of Eshelby's equivalent inclusion and Mori–Tanaka's mean field theory are used to predict the effective electroelastic properties of polycrystalline ferroelectric ceramics with aligned defects, taking the effects of the shapes of individual crystal and defect into consideration. Some numerical results for $BaTiO_3$ polycrystalline ceramics with aligned defects are carried out in order to illustrate the effects of the domain switching and defects on the effective electroelastic properties of polycrystalline ferroelectric ceramics. It has been shown that the simulations are in good agreement with the experimental results.

Keywords: Ferroelectric ceramics; Electroelastic properties; Micromechanics; Defects

1. Introduction

Due to inherent and good characteristics of piezoelectricity and pyroelectricity etc., the ferroelectric ceramics are commonly used for design as ultra-precise displacement transducers and actuators in the area of engineering. An increasing usage calls for more researchers to investigate in more detail the structure and properties of ferroelectric ceramics from different view points. In general, the polycrystalline ferroelectric ceramics can be obtained by sintering the compressed powers. It is the so called unpoling ferroelectric/piezoelectric ceramic with voids after cooled down to room temperature

* Corresponding author.

0020-7683/00/$ - see front matter
PII: S0020-7683(99)00179-1

(Ansgar et al., 1996; Cao and Evans, 1993). Currently, the ferroelectric ceramics exhibit non-piezoelectric isotropic behavior. In order to obtain more useful ceramics with piezoelectricity and anisotropy, it is important and necessary to employ 'poling' or 'polarizing', that is a process of application of a sufficiently strong electric field to the ferroelectric ceramics. Why can an electrical field cause the properties variation of the ceramics? Many scientists (Chueng and Kim, 1987; Zenon, 1994) have found the particular microscopic mapping and characteristics of the domain structures of $BaTiO_3$ and PZT ceramics by the ways of chemical etching and X-ray respectively. It is well known that a ferroelectric crystal can be divided into some regions called domain below Curie temperature, in which the polarization is arranged in the same direction, and forms a spontaneous electric polarization and strain field. The interface between two adjacent domains is called a domain wall, which includes two types: 180 and 90° domain walls. Moreover, the application of suitable external electric or mechanical field can cause 180 and 90° domain switching. An electric field can reorient both 180 and 90° domain, but a mechanical field only induces 90° domain switching. Domain switching is a complicated process that includes new domain nucleation and domain wall motion so as to minimize energy of a body under an action of external field. As a result of domain switching, the effective polarization of the overall individual crystal, which is defined as the vector sum of each domain inside the crystal without loss in generality, is approximated to the polarizing electrical field direction and then results in the effective properties change of overall ceramics. Additionally, during the poling and application microcracks will originate from the domain switching induced internal stress redistribution and act on the domain switching, which can improve (or prevent) the domain switching as shown previously (Jaff et al., 1971; Chueng and Kim, 1987; Zenon, 1994; Cao and Evans, 1993; Ansgar et al., 1996; Lynch et al., 1995; Uchida and Ikeda, 1968; Poile, 1975; Furuta and Uchino, 1993; Hideaki et al., 1994; Yang and Suo, 1994; Kahn, 1985; Zhang et al., 1997). For instance, Hideaki et al. (1994) observed that the magnitude of the electric-induced strain of PNNZT ceramics was increased by 20–40% in all samples due to the microcrack propagation, as shown in Fig. 1. Hence, domain switching is well known to be the main source of not only nonlinear deformation (Cao and Evans, 1993; Ansgar et al., 1996) like the butterfly shape but also the aging and damaging characteristics (Lynch et al., 1995; Uchida and Ikeda, 1968; Poile, 1975; Furuta and Uchino, 1993; Hideaki et al., 1994; Yang and Suo, 1994; Kahn, 1985; Zhang et al., 1997) of ferroelectric ceramics. Because of an increasing application of ferroelectric ceramics in the field of engineering, the reliability of ferroelectric structure plays a more important role. In theory, many papers have analyzed the effective moduli of linear piezoelectric ceramic without considering the effects

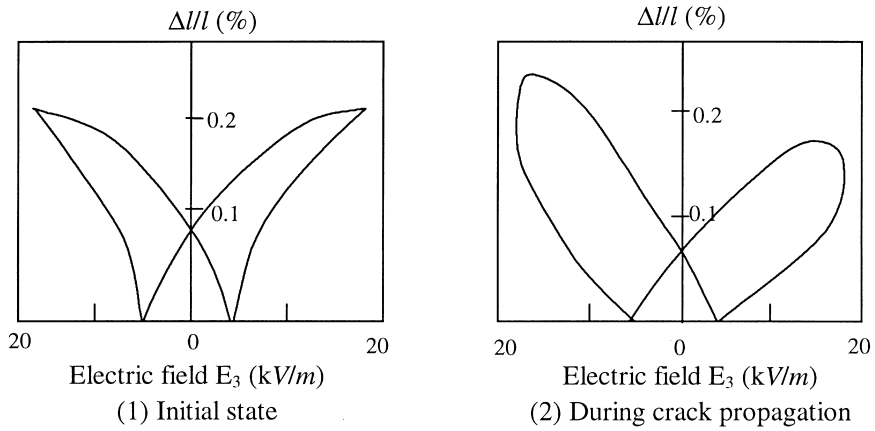

Fig. 1. The experimental results of electric induced strain changes during crack propagation (Hideaki et al., 1994).

of the inherent microstructural changes of ferroelectric ceramics under the action of an external field (Dunn and Taya, 1993a; Wang, 1994; Marutak, 1965). Kuo and Huang (1997) and Nan and Clarke (1996) studied the effective moduli of fully bonded piezoelectric ceramic, taking the effects of shape and orientations of individual crystals into account. Dunn (Dunn, 1995; Dunn and Taya, 1993b) adopted micromechanical method in order to predict effective moduli of unpoled polycrystalline piezoelectric ceramics with defects. Their works have not considered the fact that the macroscopic qualities of ferroelectric ceramics are associated with the microstructure level phenomenon, the domain switching occurs under the influence of external electric or mechanical field. Recently, Chen et al. (1997) had established a mesoscopic model to investigate the constitutive behavior of monocrystalline ferroelectrics. Hwang et al. (1995) developed a one-dimension model to analyze the relation between domain switching and electroelastic properties for ferroelectric/ferroelastics.

In this work, in terms of the phenomenological theoretical description of the domain switching process, a statistical micromechanics model is proposed in order to study the effective electroelastic properties of polycrystalline ferroelectric ceramics with aligned defects using the Eshelby–Mori–Tanaka's concept.

2. Basic equations and notations

In the case of the absence of body forces and free charge, the relationships between the static elastic and electric field can be employed on the basis of the equations of elastic equilibrium and Gauss's law of electrostatics among the strain ε_{ij}, stress ε_{ij}, electric field E_i, elastic displacement u_i, electric potential Φ and electric displacement D_i as presented in the following equations:

Divergence equations:

$$\sigma_{ij,j} = 0$$

$$D_{i,i} = 0 \tag{1}$$

Gradient equations:

$$\varepsilon_{ij} = \frac{1}{2}(u_{i,j} + u_{j,i})$$

$$E_i = -\phi_{,i} \tag{2}$$

Constitutive equations:

$$\sigma_{ij} = C_{ijmn}\varepsilon_{mn} + e_{nij}\phi_{,n}$$

$$D_i = e_{imn}\varepsilon_{mn} - k_{in}\phi_{,n} \tag{3}$$

where C_{ijmn} is the elastic modulus (measured in constant electric field), e_{nij} is the piezoelectric modulus (measured at constant strain or electric field), and k_{in} is the dielectric modulus (measured at a constant strain), respectively. It is clear that these material coefficients are instantaneous constants and affected by the applied external electric and mechanical field.

According to the notation introduced by Barnett and Lothe (1975), we can conveniently merge the above mentioned equations as:

$$Z_{Mn} = \begin{cases} \varepsilon_{mn} & M = 1, 2, 3 \\ \phi_{,n} & M = 4 \end{cases} \tag{4}$$

where Z_{Mn} is derived from U_M given by

$$U_M = \begin{cases} u_m & M = 1, 2, 3 \\ \phi & M = 4 \end{cases} \tag{5}$$

Similarly the stress and the electric displacement are represented as:

$$\Sigma_{i,J} = \begin{cases} \sigma_{ij} & J = 1, 2, 3 \\ D_i & J = 4 \end{cases} \tag{6}$$

Then, the electroelastic moduli can also be represented as:

$$E_{iJMn} = \begin{cases} C_{ijmn} & J, M = 1, 2, 3 \\ e_{nij} & J = 1, 2, 3; M = 4 \\ e_{imn} & J = 4; M = 1, 2, 3 \\ -k_{in} & J, M = 4 \end{cases} \tag{7}$$

It is noted that the 'inverse' of E_{iJMn} is defined as F_{AbiJ}, evidently E_{iJMn} and F_{AbiJ} are diagonally symmetric for common piezoelectric ceramics.

In order to conveniently derive the equation, we can represent Eqs. (4)–(7) as 9×1 and 9×9 matrices by utilizing the mapping of adjacent indices, e.g., $(iJ) = (Ji)$ and $(Mn) = (nM)$ for J and $M \neq 4$:

$$(11) \rightarrow 1, (22) \rightarrow 2, (33) \rightarrow 3, (23) \rightarrow 4, (13) \rightarrow 5, (12) \rightarrow 6, (14) \rightarrow 7, (24) \rightarrow 8, (34) \rightarrow 9.$$

Based upon the mapping, we can simplify the above expressions as matrixes in order to derive the prediction equations more easily. Then, the constitutive equations are usually presented as:

$$\Sigma_{9\times1} = E_{9\times9} Z_{9\times1}$$

$$Z_{9\times1} = F_{9\times9} \Sigma_{9\times1}$$

3. The micromechanical statistics model for polycrystalline ferroelectric ceramics with aligned defects

As it is well known, one crystal is consisted of many domains below the Curie temperature. The effective polarization of individual grain can be generally regarded as the vector sum of the polarization of each domain inside it. Before being poled, the polarization of each crystal is randomly arranged so that the overall ferroelectric ceramics exhibit isotropic and non-piezoelectric characteristics, as presented in Fig. 2(a). But under the application of a sufficiently strong electric or mechanical field, the new domain forms or the domain wall moves, so called domain switching. As a consequence of domain switching, the polarization of each grain will approximate the direction of the poling electric field so as to minimize the body energy, as shown in Fig. 2(b). Thus, the polarization means a distribution of the poling electric field direction. Merz (1956) observed the relationship between the microstructural evolution and the macroscopic response through the experimental results of $BaTiO_3$ and further concluded that domain switching is predominantly a nucleation problem. Based on the classic phase transformation statistical theory, the probability of the domain switching can be described (Merz, 1956) as

$$P = P_0 \exp\left(-\frac{b}{E} \right) \tag{8}$$

where b is the threshold constant, treated as the critical domain switching electric field. P_0 is the probability of nucleation (domain switching) for infinite field strength E. For $BaTiO_3$ ceramics, the threshold constant b is 470 kV/m. The probability of the domain switching determined by Eq. (8) only depends on the applied electric field. Under the action of the external mechanical field, we can roughly 'transfer' the applied mechanical field into the relative electric field through the piezoelectric constitutive equations in order to use the Eq. (8).

Therefore, the volume fraction of the new-switched crystal will increase in some direction as the applied external field increases. If it is assumed that there are total N potential switchable domains in volume V, the average number n of the new-switched crystal for a given electric field is

$$n = N \bullet P \tag{9}$$

Then, the volume fraction of the new-switched grains can be obtained by:

$$V_{\mathrm{f}} = n \bullet \frac{v}{V} = (Nv/V) \bullet P = V_f^0 \bullet P \tag{10}$$

where V_{f}^0 is the volume fraction of all the potential switchable crystals and v is the individual crystal volume.

Further, we depict the theoretical model of the polycrystalline ferroelectric ceramics with defects in Fig. 3. On the basis of the Eshelby's equivalent inclusion principle, we regard the new-switched crystal and spatially distributed defect as two phase inclusions ($r = 1, 2$). Then, the mean field of the matrix with electroelastic moduli E_m may differ from Σ^0 by a disturbed field Σ', caused by the presence of inclusions, and is given by

$$\Sigma_m = \Sigma^0 + \Sigma' = E_m\left(Z^0 + Z'\right) \tag{11}$$

Since the inclusions are now embedded in the matrix, for the first phase inclusion the new switched crystal, with electroelastic constants E_1, occupies a region Ω_1, and their local coordinate system is consistent with the fixed or material coordinate system as result of the domain switching. Then, we can present the electroelastic field inside the switched domain as

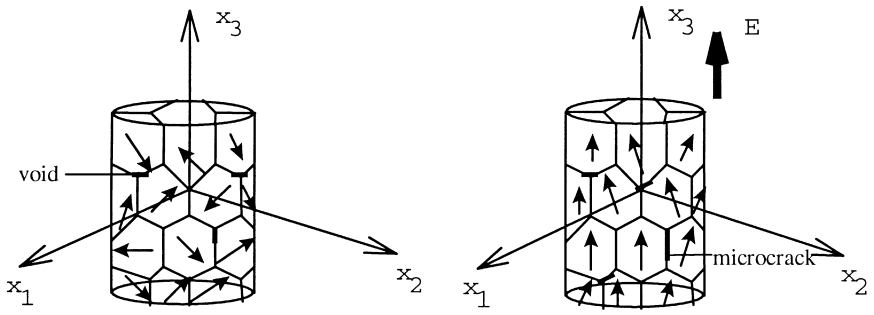

(a) unpoled ferroelectric ceramics (b) poled ferroelectric ceramic

Fig. 2. The schematic diagrams show the unpoled (a) and poled (b) ceramics and individual domain switching under the action of external field.

$$\Sigma_{in} = \Sigma^0 + \Sigma' + \Sigma_1 = E_1\left(Z^0 + Z' + Z_1 - Z_1^*\right) = E_m\left(Z^0 + Z' + Z_1 - Z_1^* - Z_1^{**}\right) \tag{12}$$

where Z_1^* is the spontaneous eigenfield: strain and electric field. Z_1^{**} is the fictitious eigenfield due to the inhomogeneity.

For the second phase inclusion, we can also give the average field in the defect which occupies the region Ω_2 by the way of Eshelby's equivalent theory in the local coordinate system:

$$\Sigma_2^L = \Sigma^{0L} + \Sigma'^{L} + \Sigma_2^L = 0 = E_m\left(Z^{0L} + Z'^{L} + Z_2^L - Z_2^{*L}\right) \tag{13}$$

where the superscript L denotes the local coordinate system. For the unidirectional aligned defects, we can assume that the fixed coordinate system is denoted as (x_1, x_2, x_3) shown in Fig. 3. The local coordinate system can be established by (x_1^L, x_2^L, x_3^L), where x_3^L represents the symmetric axis (i.e. fixed coordinate) and enables x_1^L to lie in (x_1, x_2) plane with no loss in generality. Then, we can obtain the transformation matrix T from the fixed to the local coordinate system:

$$T_{ij} = \begin{bmatrix} \cos\alpha & \sin\alpha & 0 \\ -\sin\alpha\cos\beta & \cos\alpha\cos\beta & \sin\beta \\ \sin\alpha\sin\beta & -\sin\beta\cos\alpha & \cos\beta \end{bmatrix}$$

then

$$\varepsilon_{ij}^L = T_{im}T_{jn}\varepsilon_{mn}$$

$$E_i^L = T_{in}E_n \tag{14}$$

According to the second part introduced notations, Eq. (14) can be simply re-written by

$$Z^L = [A]Z \tag{15}$$

where the transformation matrix $[A]$ is explained in detail in Appendix A.

In accordance with Wang's (1992) three-dimensional solution for an ellipsoidal inclusion in a piezoelectric material (see Appendix B), Z_r, the disturbed field about the two phase inclusions ($r = 1$, 2), can be obtained as:

$$Z_1 = S_1\left(Z_1^* + Z_1^{**}\right)$$

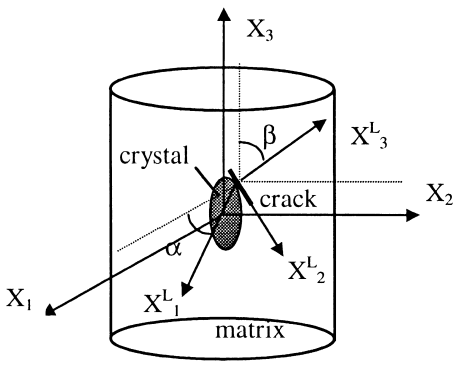

Fig. 3. A theoretical model for polycrystalline ferroelectric ceramics with the penny-shape crack.

$$Z_2^L = S_2 Z_2^{*L} \tag{16}$$

Then by the transformation matrix $[A]$:

$$Z_2 = [A]^{-1} S_2 [A] Z_2^* \tag{17}$$

Substituting Eq. (16) into Eqs. (12) and (13) yields:

$$Z_1^{**} = \left[E_1 S_1 - E_m (S_1 - I)\right]^{-1} (E_m - E_1)\left[Z^0 + Z' + (S_1 - I) Z_1^*\right] \tag{18a}$$

$$Z_2^{*L} = -(S_2 - I)^{-1}\left(Z^{0L} + Z'^{L}\right) \tag{18b}$$

Based on the transformation principles, we can obtain:

$$Z_2^* = -[A]^{-1}(S_2 - I)^{-1}[A]\left(Z^0 + Z'\right) \tag{19}$$

When the ferroelectric ceramics are subjected to a far-field traction and electric displacement, $\Sigma_{ij}^0 n_i$, on the boundary with the outward normal unit vector n_i, in accordance with the Mori–Tanaka's mean field concept, the average field of overall ceramics can be presented by

$$\begin{aligned}\langle \Sigma \rangle &= \frac{1}{V}\int_{D-\Omega_1-\Omega_2} \Sigma_m \, \mathrm{d}v + \frac{1}{V}\int_{\Omega_1} \Sigma_1 \, \mathrm{d}v + \frac{1}{V}\int_{\Omega_2} \Sigma_2 \, \mathrm{d}v = \Sigma^0 \\ &= \frac{1}{V}\int_{D-\Omega_1-\Omega_2} E_m\left(Z^0 + Z'\right) \mathrm{d}v + \frac{1}{V}\int_{\Omega_1} E_m\left(Z^0 + Z' + Z_1 - Z_1^* - Z_1^{**}\right) \mathrm{d}v + \frac{1}{V} \\ &\quad \int_{\Omega_2} E_m\left(Z^0 + Z' + Z_2 - Z_2^*\right) \mathrm{d}v\end{aligned} \tag{20}$$

then

$$0 = \frac{1}{V}\int_{D-\Omega_1-\Omega_2} E_m Z' \, \mathrm{d}v + \frac{1}{V}\int_{\Omega_1} E_m\left(Z' + Z_1 - Z_1^* - Z_1^{**}\right) \mathrm{d}v + \frac{1}{V}\int_{\Omega_2} E_m\left(Z' + Z_2 - Z_2^*\right) \mathrm{d}v \tag{21}$$

In the case of unidirectional aligned defects, the perturbed field Z' can be derived as:

$$Z' = -v_1(S_1 - I)\left(Z_1^* + Z_1^{**}\right) - v_2[A]^{-1}(S_2 - I)[A] Z_2^* \tag{22}$$

Thus, combining Eq. (19) to Eq. (22) leads to

$$Z' = \frac{1}{1 - v_2}\left[v_2 Z^0 - v_1(S_1 - I)\left(Z_1^* + Z_1^{**}\right)\right] \tag{23}$$

Eq. (23) suggests that Z' is independent of Z_2^*. Substituting Eq. (23) into Eq. (18a) gives Z_1^{**} as

$$Z_1^{**} = \left[E_1 S_1 - E_m(S_1 - I) + \frac{v_1}{1 - v_2}(E_m - E_1)(S_1 - I)\right]^{-1}(E_m - E_1)\left[\frac{1}{1 - v_2}Z^0 + \frac{1 - v_1 - v_2}{1 - v_2}(S_1 - I)Z_1^*\right] \tag{24}$$

Therefore, it is easy to derive the expression of Z_2^* in terms of Eq. (24).

Further, the overall strain and electric field denoted by $\langle Z\rangle$ can be obtained as the weighted average of each phase

$$\langle Z\rangle = \frac{1}{V}\left[\int_{D-\Omega_1-\Omega_2}\left(Z^0 + Z'\right)\mathrm{d}v + \int_{\Omega_1}\left(Z^0 + Z' + Z_1 - Z_1^*\right)\mathrm{d}v + \int_{\Omega_2}\left(Z^0 + Z' + Z_2\right)\mathrm{d}v\right] = Z^0 + v_1 Z_1^{**} + v_2\langle Z_2^*\rangle \tag{25}$$

Now combining Eqs. (10), (23) and (24) to Eq. (25), we can obtain the predicting equation about the effective macroscopic electroelastic behavior, taking the effects of domain switching and defects into consideration as following:

$$\langle \Sigma\rangle = E^*\langle Z\rangle = \Sigma^0 \tag{26}$$

Based on the above presented model analysis, it is easy for us to analyze the relation between the microstructural domain switching and the macro-response of polycrystalline ferroelectric ceramics in the next section.

4. Simulation and discussion

In this section, we will use the proposed model to analyze the effective properties of $BaTiO_3$ ceramics with aligned defects. At room temperature, $BaTiO_3$ crystal has a tetragonal phase with the particular structure parameters, such as cell constants $a = 3.992$ Å and $c = 4.035$ Å, spontaneous polarization $P_s = 0.26\ \mathrm{C/m^2}$ and remnant polarization $P_r = 0.08\ \mathrm{C/m^2}$. Then, the spontaneous eigenstrain and

Table 1
The elastic, piezoelectric and dielectric coefficients of $BaTiO_3$ at 25°C (Jaff et al., 1971)

	Single-crystal	Ceramic
C_{11}^E (GPa)	275	166
C_{33}^E (GPa)	164.8	162
C_{44}^E (GPa)	54.3	43
C_{12}^E (GPa)	178.9	77
C_{13}^E (GPa)	151.6	78
e_{31} (C m^{-2})	−2.69	−4.4
e_{33} (C m^{-2})	3.65	18.6
e_{15} (C m^{-2})	21.3	11.6
k_{11} ($\times 10^{-9}$ C^2 N^{-1} m^{-2})	17.4	11.2
k_{33} ($\times 10^{-9}$ C^2 N^{-1} m^{-2})	0.96	12.6
d_{31} ($\times 10^{-12}$ C/N)	−34.5	−79
d_{33} ($\times 10^{-12}$ C/N)	85.6	191
d_{15} ($\times 10^{-12}$ C/N)	392	270

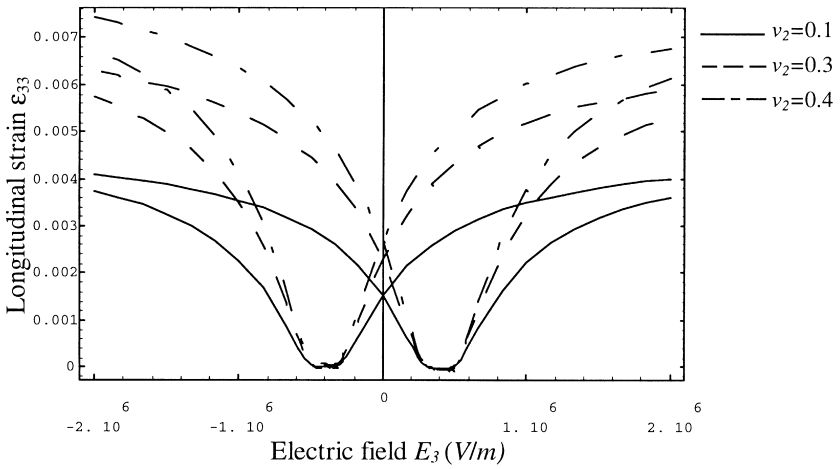

Fig. 4. The simulated strain versus the electric field for $BaTiO_3$ ceramics with aligned defects in the case of the orientation angle $\alpha = \beta = 0^\circ$.

eigenelectric displacement of single crystal can be calculated as: $\varepsilon_{11}^* = \varepsilon_{22}^* = -0.005$, $\varepsilon_{33}^* = 0.01$, $D_{33}^* = 0.26\ C/m^2$, and others are zero. The elastic, piezoelectric and dielectric coefficients of single-crystal and overall ceramics of $BaTiO_3$ are shown in Table 1.

In accordance with the material constants of $BaTiO_3$ and the statistical micromechanics model, we estimate the effects of the microstructural evolution and defects on the effective properties of polycrystalline ferroelectric ceramics. Fig. 4 shows the electric-induced strain as a function of the volume fraction v_2 of defects in the case of $\alpha = \beta = 0$. Evidently, the magnitude of the electric-induced strain increases with the volume fraction v_2 of the defects increasing, as shown in Fig. 4. In addition, the distribution of the defects also influences significantly on the electric-induced strain, as shown in Fig. 5. From Fig. 5, it is obvious that the effect of defects in some directions on the magnitude of the electric-

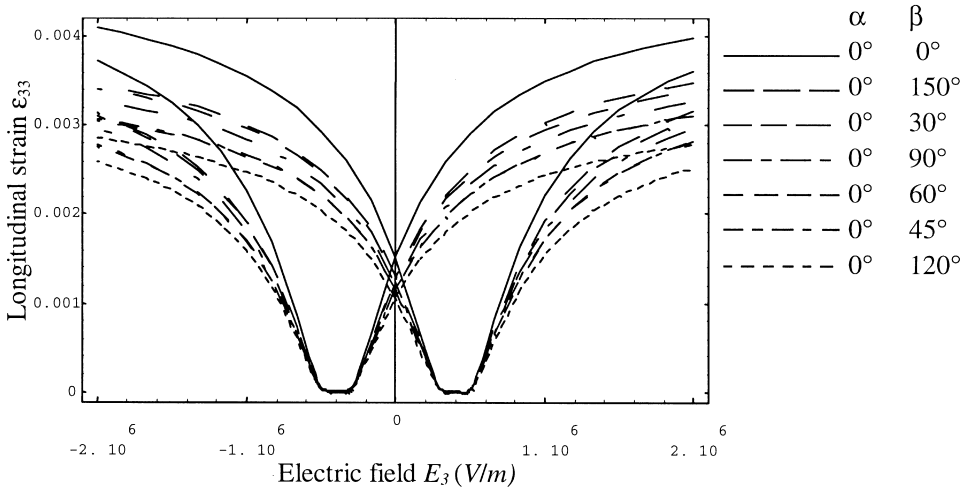

Fig. 5. The calculated strain versus the electric field for $BaTiO_3$ ceramics with aligned defects in the case of the volume fraction $v_2 = 0.1$.

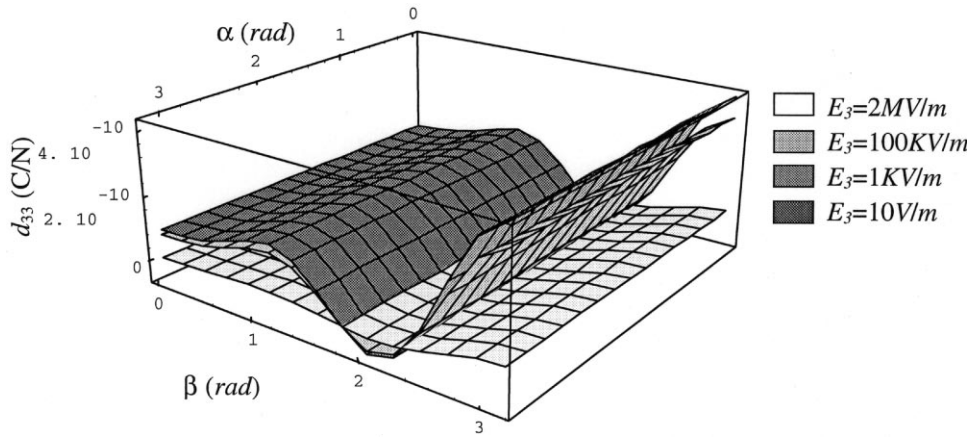

Fig. 6. The effects of the external applied electric field E_3 and the defect orientation angle on the effective piezoelectric modulus d_{33} in the case of $v_2 = 0.01$ and free from compressive stress.

induced strain is more profound than that in other directions. The simulations shown in Figs. 4 and 5 reveal that the predicted electric vs. strain curves exhibit a butterfly non-symmetric loop about the axis of $E_3 = 0$ V/m. It is suggested that the magnitude of the electric-induced strain under the application of the negative electric field E_3 is greater than that under the action of positive electric field, and, the increase of the magnitude possibly exceeds 20–40%, as the experimental observations from Fig. 1 (Hideaki et al., 1994).

Further, the predictions of the effective piezoelectric modulus d_{33} are presented in Figs. 6–8 as a function of the applied external field, the distribution and the volume fraction v_2 of defects, respectively. To the effect of the defect distribution on the piezoelectric constant, the simulations of d_{33} are shown in Figs. 6–8. We can see that d_{33} will increase to the peak at $\beta \approx 60^\circ$, then decrease to a minimum at $\beta = 119.4^\circ$ and gradually arrive at $\beta = 180^\circ$ for a given external field and volume fraction of defects. As predicted, the predictions of d_{33} will be reduced with increasing the applied external electric field or

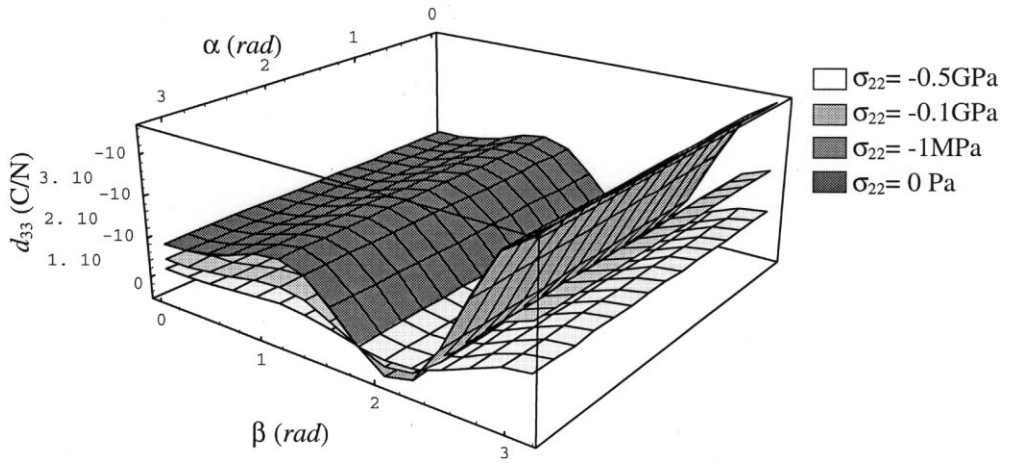

Fig. 7. The effects of external stress field and orientation angle of defects on the effective piezoelectric modulus d_{33} in the case of $v_2 = 0.01$ and electric field $E_3 = 100$ kV/m.

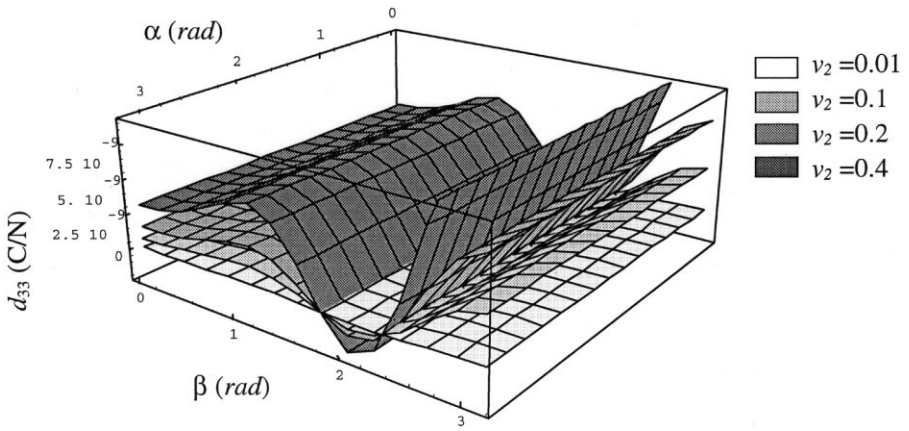

Fig. 8. The effects of the volume fraction v_2 and orientation angle of the defects on the effective piezoelectric modulus d_{33} in the case of elec1tric field $E_3 = 100$ kV/m and free from stress.

compressive stress when the orientation angle β is within the regions of 0–102° and 138.7–180° in any case of $\alpha = 0$–180°. In contrast, d_{33} increases with the external electric field increasing in the case of $\beta =$ 102–138.7°. Fig. 8 shows the variation of piezoelectric modulus with the volume fraction of defects in constant external fields. Obviously, the values of d_{33} increase with the volume fraction v_2 of the aligned defects increasing, when the orientation angle β of defects is in the ranges of 0–102° and 138.7–180°, but decrease in the case of $\beta = 102$–138.7°.

Similarly, the calculations of the effective elastic modulus S_{23} presented in Figs. 9–11 indicate that the effective elastic modulus S_{23} is also greatly affected by the applied external field and defects. From Figs. 9 and 10, we can see that the simulations of S_{23} also increases nonlinearly in the case of the orientation angle β ranging within 0–102° and 138.7–180°, but reduce in the region of $\beta = 102$–138.7°, as the external electric field or compress stress increases. The influence of the volume fraction v_2 of defects on the elastic modulus is depicted in Fig. 11. This suggests that the values of S_{23} will reduce more

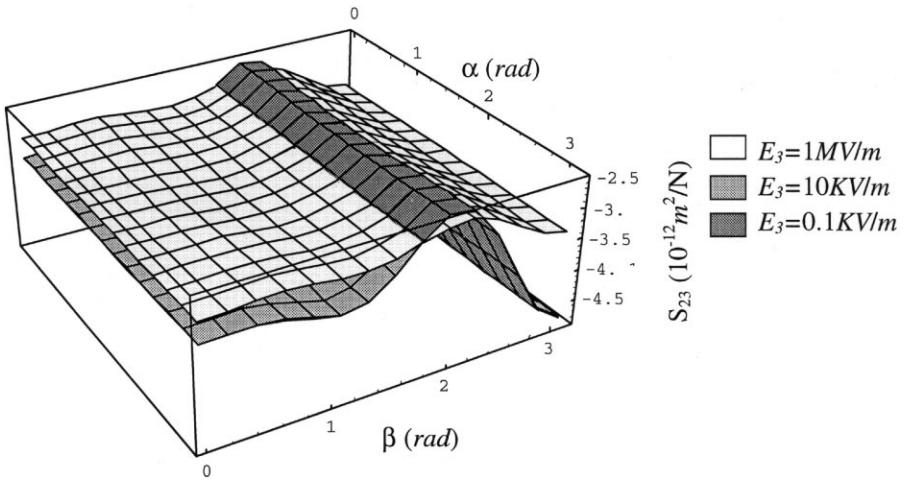

Fig. 9. The effects of applied electric field E_3 and defect orientation on the effective elastic modulus S_{23} in the case of $v_2 = 0.01$ and free from stress.

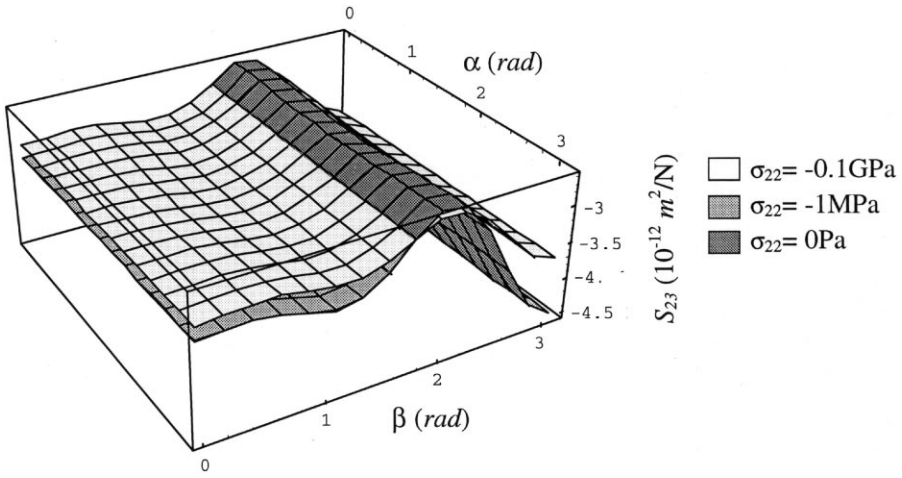

Fig. 10. The influences of external applied stress and defect orientation on the effective elastic modulus S_{23} in the case of $v_2 = 0.01$ and applied electric field $E_3 = 100$ KV/m.

obviously in the case that β is in the ranges of 0–102° and 138.7–180° but rise in the case of β within the region of 102–138.7°, when the volume fraction v_2 of the initial defects increases.

All the predictions shown in Figs. 6–11 reveal that the applied external field and defects can induce substantial changes in the electroelastic properties of polycrystalline ferroelectric ceramics, which are attributed to domain switching. Since the enhancement of the applied external field causes the domain switching, the domain switching results in rearranging the internal stress around the defect and then leads to the defects in some orientations tending to propagate but close in other orientations. Hence, the changes of the effective electroelastic properties of polycrystalline ferroelectric ceramics are not

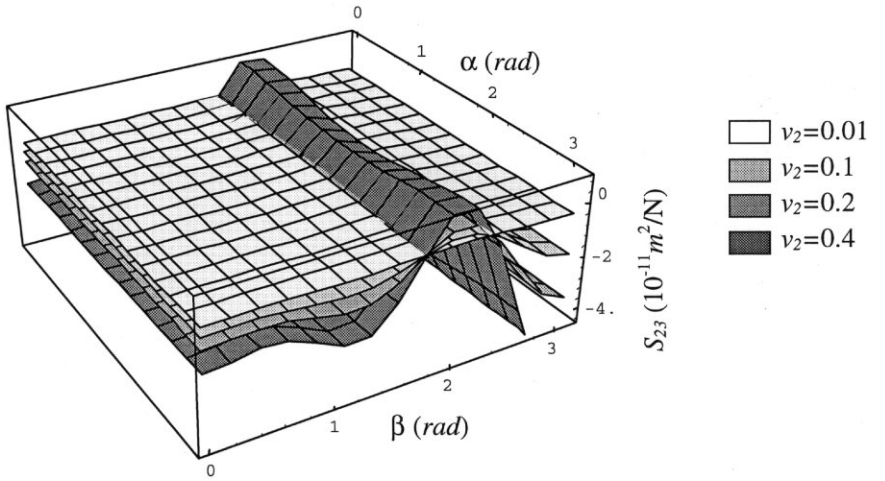

Fig. 11. The effects of the volume fraction v_2 and orientation of the defects on the effective elastic modulus S_{23} at constant electric field $E_3 = 100$ KV/m.

consistent with the variation of the orientation angle β. Then, we can see that the defect in some direction will improve the piezoelectric properties but reduce the elastic properties, as shown in Figs. 6–11. On the other hand, the higher the applied external field, the less distinct the effects of the applied external field on the effective electroelastic properties under a given condition. With increasing the applied external field, less and less domains can switch. Thus, the interaction between the defects and domain switching will decline so that the effect shows a reductive state, which is evidently presented in Figs. 6–11.

5. Conclusion

In terms of the phenomenological theory and the characteristics of the microstructural evolution of the ferroelectric ceramics, a statistical micromechanics model was developed to describe the evolution characteristics of the domain switching. Further, the ways of Eshelby–Mori–Tanaka's theory and Wang's three-dimensional solution of an ellipsoidal inclusion embedded in a piezoelectric matrix was adopted to predict the effective behavior of polycrystalline ferroelectric ceramics with aligned defects. Based on the analysis about the $BaTiO_3$ ceramics, it was found that the domain switching decided the effective properties of polycrystalline ferroelectric ceramics under the action of applied external field, and the defects can improve the piezoelectric properties but degrade the elastic properties in some cases. These predictions are consistent with the experimental results.

Acknowledgements

This work was supported by the National Foundation of China for Excellent Young Investigators.

Appendix A

The components of $[A]$ matrix are shown as:

$$ff = \begin{bmatrix} nn & mm & 0 & 0 & 0 & 2nm \\ mmpp & nnpp & qq & 2npq & -2mpq & -2nmpp \\ mmqq & qqnn & pp & -2npq & 2mpq & -2mnqq \\ -pqmm & -pqnn & pq & npp - nqq & mqq - mpp & nmpq \\ nmq & -nmq & 0 & mp & np & qmm - qnn \\ -nmp & nmp & 0 & mq & nq & pnn - pmm \end{bmatrix}$$

and

$$fe = \begin{bmatrix} n & m & 0 \\ -mp & np & q \\ mq & -nq & p \end{bmatrix}$$

where $n = \cos\alpha$, $m = \sin\alpha$, $p = \cos\beta$, $q = \sin\beta$, 'ff' is a 6×6 matrix and 'fe' is a 3×3 matrix.

Then,

$$A = \begin{bmatrix} ff & 0_{6\times3} \\ 0_{3\times6} & fe \end{bmatrix}$$

and

$$A^{\mathrm{T}} = A^{-1}$$

Appendix B

Consider an infinite piezoelectric body with the elastic moduli C^0, the piezoelectric moduli e^0 and dielectric permitivity k^0 in which there is an inhomogeneous inclusion occupying a region Ω with constants C, e and k, by introducing the following notations:

$$C^1_{ijkl} = C_{ijkl} - C^0_{ijkl} \tag{B1}$$

$$e^1_{mij} = e_{mij} - e^0_{mij} \tag{B2}$$

$$k^1_{kl} = k_{kl} - k^0_{kl} \tag{B3}$$

So the electroelastic constant tensors of the inhomogeneous medium can be written as:

$$C_{ijkl}(x) = C^1_{ijkl}h(x) + C^0_{ijkl}(x) \tag{B4}$$

$$e_{mij}(x) = e^1_{mij}h(x) + e^0_{mij}(x) \tag{B5}$$

$$k_{kl}(x) = k^1_{kl}h(x) + k^0_{kl}(x) \tag{B6}$$

where $h(x)$ is the characteristic function and is defined by:

$$h(x) = \begin{cases} 1 & x \in \Omega \\ 0 & \text{otherwise} \end{cases} \tag{B7}$$

Substitution of Eqs. (B3)–(B5) into divergence Eq. (1) and constitutive Eq. (3) yields:

$$C^0_{ijkl}u_{k,lj} + e^0_{mij}\phi_{,mj} = -\left[C^1_{ijkl}u_{k,l}h(x)\right]_{,j} - \left[e^1_{mij}\phi_{,m}h(x)\right]_{,j} \tag{B8}$$

$$e^0_{mij}u_{i,jm} - k^0_{ml}\phi_{,lm} = -\left[e^1_{mij}u_{i,j}h(x)\right]_{,m} + \left[k^1_{ml}\phi_{,l}h(x)\right]_{,m} \tag{B9}$$

Based on the fictitious eigenstrain ε^*_{ij} and eigenelectric field E^*_i due to inhomogeneity, then Eqs. (B8) and (B9) can be expressed as:

$$C^0_{ijkl}u_{k,lj} + e^0_{mij}\phi_{,mj} = \left[\left(C^0_{ijkl}u^*_{k,l} + e^0_{mij}\phi^*_{,m}\right)h(x)\right]_{,j} \tag{B10}$$

$$e^0_{mij}u_{i,jm} - k^0_{ml}\phi_{,lm} = \left[\left(e^0_{mij}u^*_{i,j} - k^0_{ml}\phi^*_{,l}\right)h(x)\right]_{,m} \tag{B11}$$

By introducing the Green's functions G^1, G^2, F^1, F^2 as follows:

$$C^0_{ijkl}G^1_{kp,lj} + e^0_{mij}F^1_{p,mj} = -\delta_{ip}2\delta(x-x')$$

$$e^0_{jkl}G^1_{kp,lj} - k^0_{jk}F^1_{p,jk} = 0$$

$$C^0_{ijkl}G^2_{k,lj} + e^0_{kij}F^2_{,kj} = 0$$

$$e^0_{jkl}G^2_{k,lj} - k^0_{jk}F^2_{,jk} = -\delta(x-x') \tag{B12}$$

Fourier transform of Eq. (B10) can be obtained easily and expressed in the fourth-order matrix form as:

$$\begin{bmatrix} C^0_{ijkl}\xi_l\xi_j & e^0_{kij}\xi_k\xi_j \\ e^0_{jkl}\xi_l\xi_j & -k^0_{jk}\xi_k\xi_j \end{bmatrix}\begin{bmatrix} G^{1T}_{kp} & F^{1T}_{p} \\ G^{2T}_{k} & F^{2T} \end{bmatrix} = \begin{bmatrix} \delta_{ip} & 0 \\ 0 & 1 \end{bmatrix} \tag{B13}$$

Where

$$G^1_{kl}(x-x') = \frac{1}{(2\pi)^3}\int G^{1T}_{kp}(\xi)\exp\left[i\xi(x-x')\right]\mathrm{d}\xi$$

and G^{2T}_k, F^{1T}_p and F^{2T} can be determined similarly.

$$G^1_{kp,ij}(x-x') = -\frac{1}{(2\pi)^3}\int G^{1T}_{kp}(\xi)\xi_i\xi_j\exp\left[i\xi(x-x')\right]\mathrm{d}\xi$$

Based on Eq. (B13), the elastic displacement u_m, electric potential ϕ, strain field and electric field can be obtained easily. Following the same procedure as Mura (1987) in deriving the elastic field of an anisotropic, ellipsoidal inclusion in non-piezoelectric media, basing on gradient Eq. (2), the elastic field and electric field inside the piezoelectric inclusion can be obtained as following:

$$\varepsilon^I_{\alpha\beta} = \frac{1}{(2\pi)^3}\left[\left(N^1_{\alpha i\beta j} + N^1_{\beta i\alpha j}\right)\left(C^0_{ijkl}u^*_{k,l} + e^0_{mij}\phi^*_{,m}\right) + \left(N^2_{\alpha\beta j} + N^2_{\beta\alpha j}\right)\left(e^0_{mij}u^*_{i,j} - k^0_{ml}\phi^*_{,l}\right)\right] \tag{B14}$$

$$E^I_{\alpha} = -\frac{1}{4\pi}\left[N^2_{ji\alpha}\left(C^0_{ijkl}u^*_{k,l} + e^0_{mij}\phi^*_{,m}\right) + N^3_{\alpha i}\left(e^0_{mij}u^*_{i,j} - k^0_{ml}\phi^*_{,l}\right)\right] \tag{B15}$$

where

$$N^1_{ijkl} = \int_{-1}^{1}\mathrm{d}w_3\int_0^{2\pi} G^{1T}_{\alpha j}(w)w_k w_l\,\mathrm{d}\theta$$

$$N^2_{ijk} = \int_{-1}^{1}\mathrm{d}w_3\int_0^{2\pi} G^{2T}_{i}(w)w_k w_j\,\mathrm{d}\theta$$

$$N^3_{ij} = \int_{-1}^{1}\mathrm{d}w_3\int_0^{2\pi} F^{1T}(w)w_i w_j\,\mathrm{d}\theta$$

If the matrix is transversely isotropic piezoelectric material, the non-zero components of N^1, N^2, N^3 can

be obtained (these results had been presented in Wang (1992)). Then the Eshelby's electroelastic tensors can be obtained.

Based on the second part formulations, Eqs. (B14) and (B15) can be simplified as following:

$$Z^I = SZ^* \tag{B16}$$

where

$$S = \begin{bmatrix} S_{11} & S_{12} & S_{13} & S_{14} & S_{15} & 0 & 0 & 0 & S_{19} \\ S_{21} & S_{22} & S_{23} & S_{24} & S_{25} & 0 & 0 & 0 & S_{29} \\ S_{31} & S_{32} & S_{33} & S_{34} & S_{35} & 0 & 0 & 0 & S_{39} \\ S_{41} & S_{42} & S_{43} & S_{44} & S_{45} & 0 & 0 & S_{48} & 0 \\ S_{51} & S_{52} & S_{53} & S_{54} & S_{55} & 0 & S_{57} & 0 & 0 \\ 0 & 0 & 0 & 0 & 0 & S_{66} & 0 & 0 & 0 \\ 0 & 0 & 0 & 0 & S_{75} & 0 & S_{77} & 0 & 0 \\ 0 & 0 & 0 & S_{84} & 0 & 0 & 0 & S_{88} & 0 \\ S_{91} & S_{92} & S_{93} & 0 & 0 & 0 & 0 & 0 & S_{99} \end{bmatrix}$$

where components of matrix [S] can be obtained as follows:

$$S_{11} = \frac{1}{4\pi}\left(C^0_{11}N^1_{1111} + C^0_{12}N^1_{1212} + C^0_{31}N^1_{1313} + e^0_{31}N^2_{113}\right)$$

$$S_{12} = \frac{1}{4\pi}\left(C^0_{12}N^1_{1111} + C^0_{22}N^1_{1212} + C^0_{32}N^1_{1313} + e^0_{32}N^2_{113}\right)$$

$$S_{13} = \frac{1}{4\pi}\left(C^0_{13}N^1_{1111} + C^0_{23}N^1_{1212} + C^0_{33}N^1_{1313} + e^0_{33}N^2_{113}\right)$$

$$S_{14} = \frac{1}{4\pi}e^0_{24}N^2_{113}$$

$$S_{15} = \frac{1}{4\pi}e^0_{15}N^2_{113}$$

$$S_{19} = -\frac{1}{4\pi}\left(e^0_{31}N^1_{1111} + e^0_{32}N^1_{1212} + e^0_{33}N^1_{1313} - k^0_{33}N^2_{113}\right)$$

$$S_{21} = \frac{1}{4\pi}\left(C^0_{11}N^1_{2121} + C^0_{21}N^1_{2222} + C^0_{31}N^1_{2323} + e^0_{31}N^2_{223}\right)$$

$$S_{22} = \frac{1}{4\pi}\left(C^0_{12}N^1_{2121} + C^0_{22}N^1_{2222} + C^0_{32}N^1_{2323} + e^0_{32}N^2_{223}\right)$$

$$S_{23} = \frac{1}{4\pi}\left(C^0_{13}N^1_{2121} + C^0_{23}N^1_{2222} + C^0_{33}N^1_{2323} + e^0_{33}N^2_{223}\right)$$

$$S_{24} = \frac{1}{4\pi} e^0_{24} N^2_{223}$$

$$S_{25} = \frac{1}{4\pi} e^0_{15} N^2_{223}$$

$$S_{29} = -\frac{1}{4\pi}\left(e^0_{31} N^1_{2121} + e^0_{32} N^1_{2222} + e^0_{33} N^1_{2323} - k^0_{33} N^2_{223}\right)$$

$$S_{31} = \frac{1}{4\pi}\left(C^{\,0}_{11} N^1_{3131} + C^{\,0}_{21} N^1_{3232} + C^{\,0}_{31} N^1_{3333} + e^0_{31} N^2_{333}\right)$$

$$S_{32} = \frac{1}{4\pi}\left(C^{\,0}_{12} N^1_{3131} + C^{\,0}_{22} N^1_{3232} + C^{\,0}_{32} N^1_{3333} + e^0_{32} N^2_{333}\right)$$

$$S_{33} = \frac{1}{4\pi}\left(C^{\,0}_{13} N^1_{3131} + C^{\,0}_{23} N^1_{3232} + C^{\,0}_{33} N^1_{3333} + e^0_{33} N^2_{333}\right)$$

$$S_{34} = \frac{1}{4\pi} e^0_{24} N^2_{333}$$

$$S_{35} = \frac{1}{4\pi} e^0_{15} N^2_{333}$$

$$S_{39} = -\frac{1}{4\pi}\left(e^0_{31} N^1_{3131} + e^0_{32} N^1_{3232} + e^0_{33} N^1_{3333} - k^0_{33} N^2_{333}\right)$$

$$S_{41} = \frac{1}{8\pi} e^0_{31} N^2_{322}$$

$$S_{42} = \frac{1}{8\pi} e^0_{32} N^2_{322}$$

$$S_{43} = \frac{1}{8\pi} e^0_{33} N^2_{322}$$

$$S_{44} = \frac{1}{4\pi}\left[C^{\,0}_{44}\left(N^1_{3232} + N^1_{3322} + N^1_{2323} + N^1_{2233}\right) + e^0_{24}\left(N^2_{232} + N^2_{322}\right)\right]$$

$$S_{45} = \frac{1}{4\pi} e^0_{15} N^2_{322}$$

$$S_{48} = -\frac{1}{8\pi}\left[e^0_{24}\left(N^1_{3232} + N^1_{3322} + N^1_{2332} + N^1_{2233}\right) - k^0_{22}\left(N^2_{232} + N^2_{322}\right)\right]$$

$$S_{51} = \frac{1}{8\pi} e^0_{31} N^2_{311}$$

$$S_{52} = \frac{1}{8\pi} e^0_{32} N^2_{311}$$

$$S_{53} = \frac{1}{8\pi} e^0_{33} N^2_{311}$$

$$S_{54} = \frac{1}{4\pi} e^0_{24} N^2_{311}$$

$$S_{55} = \frac{1}{4\pi}\left[C^0_{55}\left(N^1_{1133} + N^1_{1313} + N^1_{3113} + N^1_{3311}\right) + e^0_{15}\left(N^2_{311} + N^2_{131}\right)\right]$$

$$S_{57} = -\frac{1}{8\pi}\left[e^0_{15}\left(N^1_{1133} + N^1_{1331} + N^1_{3113} + N^1_{3311}\right) - k^0_{11}\left(N^2_{311} + N^2_{131}\right)\right]$$

$$S_{66} = \frac{1}{4\pi} C^0_{66}\left(N^1_{1122} + N^1_{1221} + N^1_{2112} + N^1_{2211}\right)$$

$$S_{75} = -\frac{1}{2\pi}\left[C^0_{13}\left(N^2_{311} + N^2_{131}\right) + e^0_{15} N^3_{11}\right]$$

$$S_{77} = \frac{1}{4\pi}\left[e^0_{15}\left(N^2_{311} + N^2_{131}\right) - k^0_{11} N^3_{11}\right]$$

$$S_{84} = -\frac{1}{2\pi}\left[C^0_{44}\left(N^2_{322} + N^2_{232}\right) + e^0_{24} N^3_{22}\right]$$

$$S_{88} = \frac{1}{4\pi}\left[e^0_{24}\left(N^2_{322} + N^2_{232}\right) - k^0_{22} N^3_{22}\right]$$

$$S_{91} = -\frac{1}{4\pi}\left(C^0_{11} N^2_{113} + C^0_{12} N^2_{223} + C^0_{31} N^2_{333} + e^0_{31} N^3_{33}\right)$$

$$S_{92} = -\frac{1}{4\pi}\left(C^0_{12} N^2_{113} + C^0_{22} N^2_{223} + C^0_{32} N^2_{333} + e^0_{32} N^3_{33}\right)$$

$$S_{93} = -\frac{1}{4\pi}\left(C^0_{13} N^2_{113} + C^0_{23} N^2_{223} + C^0_{33} N^2_{333} + e^0_{33} N^3_{33}\right)$$

$$S_{99} = \frac{1}{4\pi}\left(e^0_{31} N^2_{113} + e^0_{32} N^2_{223} + e^0_{33} N^2_{333} - k^0_{33} N^3_{33}\right)$$

References

Ansgar, B.S., et al., 1996. Ferroelastic properties of lead zirconate titanate ceramics. J. Am. Ceram. Soc 79 (10), 2637–2640.

Barnett, D.M., Lothe, J., 1975. Dislocations and line charges in anisotropic piezoelectric insulators. Phys. Status. Solidi B (67), 105–117.

Cao, Hengchu, Evans, A.G., 1993. Nonlinear deformation of ferroelectric ceramics. J. Am. Ceram. Soc 76 (4), 890–896.

Chen, Xi., Fang, DiaNing, Hwang, Keh-Chih, 1997. A mesoscopic model of the constitutive behavior of monocrystalline ferroelectrics. Smart Mater. Struct 6, 145–151.

Chueng, H.T., Kim, H.G., 1987. Characteristics of domain in tetragonal phase PZT ceramics. Ferroelectrics 76, 327–333.

Dunn, M.L., Taya, M., 1993a. Micromechanics predictions of the effective electroelastic modulus of piezoelectric composites. Int. J. Solids Structures 30 (2), 161–3175.

Dunn, M.L., Taya, M., 1993b. Electromechanical properties of porous piezoelectric ceramics. J. Am. Ceram. Soc 76 (7), 1697–1706.

Dunn, M.L., 1995. Effects of grain shape anisotropy, porosity, and microcracks on the elastic and dielectric constants of polycrystalline piezoelectric ceramics. J. Appl. Phys 78 (3), 1533–1541.

Furuta, A., Uchino, K., 1993. Dynamic observation of crack propagation in piezoelectric multilayer actuators. J. Am. Ceram. Soc 76 (6), 1615–1617.

Hideaki, A., et al., 1994. Destruction mechanisms in ceramic mutlilayer actuators. Jpn. J. Appl. Phys 33, 3091–3094.

Hwang, S.C., Lynch, C.S., McMeeking, R.M., 1995. Ferroelectric/ferroelastic interactions and a polarization switching model. Acta Metall. Mater 43 (5), 2073–2084.

Jaff, B., Cook, W.R., Jaff, H., 1971. Piezoelectric ceramic. Academic press, New York.

Kahn, M., 1985. Acoustic and elastic properties of PZT ceramics with anisotropic pores. J. Am. Ceram. Soc 68 (11), 623–628.

Kuo, Wen Shyong, Huang, Jin H., 1997. On the effective electroelastic properties of piezoelectric composites containing spatially oriented inclusions. Int. J. Solids Structures 34 (19), 2445–2461.

Lynch, C.S., Yang, W., et al., 1995. Electric field induced cracking in ferroelectric ceramics. Ferroelectrics 166, 11–30.

Marutak, M., 1965. A calculation of physical constants of lead zirconate barium titanate. J. Phys. Soc. Jpn 11 (8), 807–814.

Merz, W.J., 1956. Switching time in ferroelectric $BaTiO_3$ and its dependence on crystal thickness. J. Appl. Phys 27 (8), 938–943.

Mura, T., 1987. Micromechanics of Defects in Solids. Martinus Nijhoff, Dordrecht (Boston).

Nan, Ce-Wen, Clarke, D.R., 1996. Piezoelectric modulus of piezoelectric ceramics. J. Am. Ceram. Soc 79 (10), 2563–2566.

Poile, N.J., 1975. Effects of aging and compressive stress on the properties of $BaTiO_3$ ceramics. J. Phy. D: Appl. Phys 8, 1140–1148.

Uchida, Naoya, Ikeda, Takuro, 1968. The aging characteristics in perovskite-type ferroelectric ceramics. Jpn. J. Appl. Phys 7 (10), 1219–1226.

Wang, Biao, 1992. Three-dimensional analysis of an ellipsoidal inclusion in a piezoelectric material. Int. J. Solids Structures 29 (3), 293–308.

Wang, Biao, 1994. Effective behavior of piezoelectric composites. Appl. Mech. Review 47 (1), 112–121.

Yang, W., Suo, Z., 1994. Cracking in ceramic actuators caused by electrostriction. J. Mech. Phys. Solids 42, 649–663.

Zenon, B., 1994. Optical microscopic mapping of the domain structure of $BaTiO_3$ Microcrystals. Ferroelectrics 157, 13–18.

Zhang, Q.M., et al., 1997. Change of the weak-field properties of $Pb(ZrTi)O_3$ piezoceramics with the compressive uniaxial stresses and its links to the effect of dopants on the stability of the polarizations in the materials. J. Mater. Res 12 (1), 226–234.